J. Fluid Mech. (2001), *vol.* 440, *pp.* 49–74. Printed in the United Kingdom

Sand bars in tidal channels. Part 1. Free bars

By G. SEMINARA[1] AND M. TUBINO[2]

[1]Dipartimento di Ingegneria Ambientale, Università di Genova,
Via Montallegro 1, 16145 Genova, Italy
e-mail: sem@diam.unige.it

[2]Dipartimento di Ingegneria Civile e Ambientale,
Università di Trento, Via Mesiano 77, 38050 Trento, Italy
e-mail: marco.tubino@ing.unitn.it

(Received 19 August 1999 and in revised form 25 January 2001)

We investigate the basic mechanism whereby bars form in tidal channels or estuaries. The channel is assumed to be long enough to allow neglect of the effects of end conditions on the process of bar formation. In this respect, the object of the present analysis differs from that of Schuttelaars & de Swart (1999) who considered bars of length scaling with the finite length of the tidal channel. The channel bottom is assumed to be cohesionless and consisting of uniform sediments. Bars are shown to arise from a mechanism of instability of the erodible bed subject to the propagation of a tidal wave. Sediment is assumed to be transported both as bedload and as suspended load. A fully three-dimensional model is employed both for the hydrodynamics and for sediment transport. At the leading order of approximation considered, the effects of channel convergence, local inertia and Coriolis forces on bar instability are shown to be negligible. Unlike fluvial free bars, in the absence of mean currents tidal free bars are found to be non-migrating features (in the mean). Instability arises for large enough values of the mean width to depth ratio of the channel, for given mean values of the Shields parameter and of the relative channel roughness. The role of suspended load is such as to stabilize bars in the large-wavenumber range and destabilize them for small wavenumbers. Hence, for large values of the mean Shields stress, it turns out that the first critical mode (the alternate bar mode) is characterized by a very small value of the critical width to depth ratio. Furthermore, the order-m mode being characterized by a critical value of the width to depth ratio equal to m times the critical value for the first mode, it follows that for large values of the mean Shields stress several unstable modes are simultaneously excited for relatively low values of the aspect ratio. This suggests that the actual bar pattern observed in nature may arise from an interesting nonlinear competition among different unstable modes.

1. Introduction

Bars are sediment waves with wavelengths scaling with channel width, which form both in fine and in coarse sediments. The subject of river bars has been widely investigated in the last decade (see Seminara 1995 for a recent review) as their formation is associated with several important fluvial processes, like river meandering and braiding.

Little attention has been devoted so far to the analogous problem concerning the formation of bars in tidal channels. The interest of this problem, which is the subject

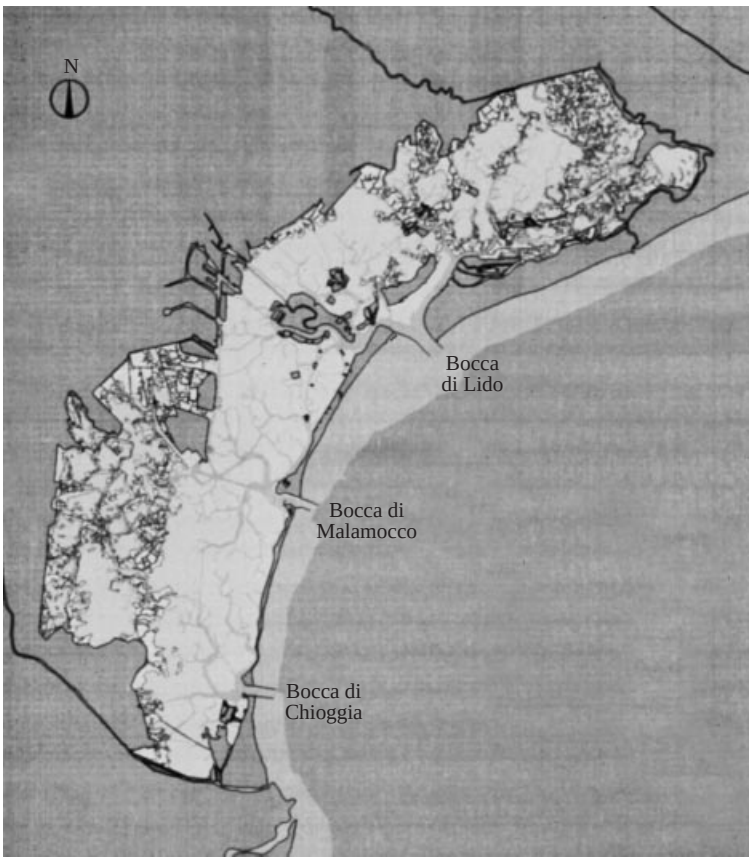

FIGURE 1. The Venice Lagoon.

of the present investigation, is both practical and conceptual. Indeed the original motivation for the present work arose in the context of a general investigation on the basic mechanisms which control the morphologic evolution of Venice Lagoon, which consists of interconnected networks of tidal channels, each network originating at one of the three lagoon inlets (figure 1). Shallow flats are adjacent to the channels, some of them being normally submerged (except during exceptionally low tides) while others normally emerge (except during exceptionally high tides). Geomorphological studies (Barwis 1978) have shown that similarities exist between the geometrical characteristics of tidal networks and those known to be typical of river basins. Tidal channels are typically meandering with meander wavelengths ranging about 6–12 channel widths and meander radii of the order of 1.5–4 channels widths (but see § 2 of Part 2 for more detailed observations). Similar values are typical of rivers. On the other hand, (Solari *et al.* 2001) while the fate of river meanders is usually 'meander cutoff', i.e. fluvial meanders do not generally reach an equilibrium configuration, in the tidal case meanders appear to be more stable. In particular the meandering configuration of the Venice tidal channels has not exhibited significant variations in the period 1930–1970.

Neither the above similarities nor the distinctive features of tidal meanders can be given an obvious mechanistic interpretation. In order to achieve some understanding it is first necessary to investigate the major unit process controlling the morphody-

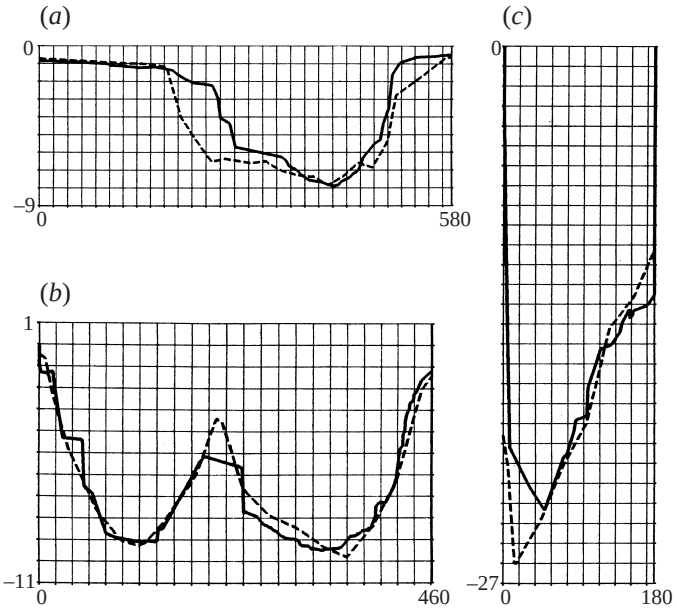

FIGURE 2. Typical channel cross-sections of Venice Lagoon: (*a*) Perognola channel (basin of Chioggia); (*b*) Treporti channel (basin of Lido); (*c*) S. Nicolò channel (basin of Lido). Dashed lines, 1970 cross-section; solid lines, 1990 cross-section.

namics of tidal channels, namely the formation of tidal bars, i.e. the development of deformations of the undisturbed uniform bottom topography which may arise either as a 'free' response, through an instability of the basic uniform flow topography, or as a 'forced' response to some forcing mechanism like channel curvature. The fact that both mechanisms do indeed operate in the context of tidal channels emerges from a glance at figure 2(*a–c*) where three typical channel cross-sections in Venice Lagoon display the presence of an alternate (free) bar, a central (free) bar and a point (forced) bar, respectively. Free bars are investigated in the present paper, while forced bars are analysed in Part 2 (Solari *et al.* 2001).

A description of the morphology of estuarine bar forms can be found in the sedimentological literature. In a recent review paper Dalrymple & Rhodes (1995) propose classifying estuarine bars into 'repetitive barforms' (i.e. alternate, point and braid bars occurring in tidal channels and creeks of estuaries), 'elongate tidal bars' (which are features characteristic of the outer part of macrotidal estuaries but are also observed at the mouth of estuaries with smaller tidal ranges) and 'delta like bodies' (isolated features typically forming where a channel widens considerably). Our present concern is with the first class of bars and more precisely with the formation of alternate 'free' bars in straight tidal channels.

We will deliberately ignore several complicating features of the real problem. In particular we will ignore the possible role of interactions between the channel and the adjacent tidal flats along with the effects of bank erodibility. We will also ignore any source of flow motion except for tide propagation. In particular, flows due to density currents, river currents and wave action will be taken to play no role. The channel length and the spatial scale of its width variations are assumed to be much larger than a typical bar wavelength. Hence the formation of bars may be investigated assuming that, at the leading order of approximation, the basic state, i.e. flow, bed topography

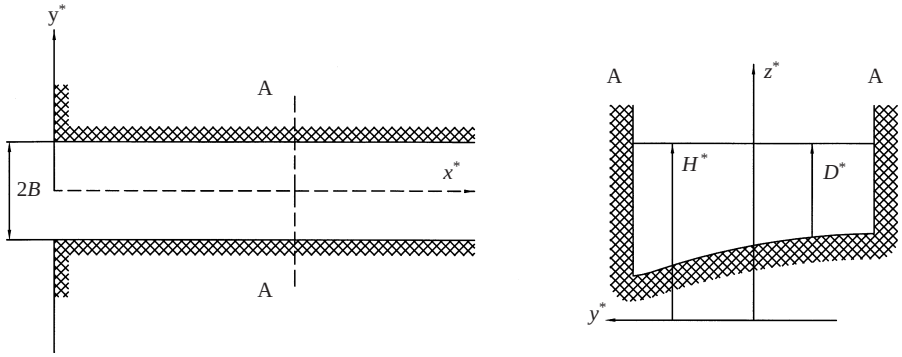

FIGURE 3. Sketch of the channel and notation.

and sediment transport associated with tide propagation in the undisturbed channel, is spatially uniform and time periodic. The stability of flow–bed topography in a long straight channel with erodible bed and non-erodible banks subject to the propagation of a tidal wave provides the simplest, yet basic, problem, to be investigated.

The stability analysis describing the formation of tidal bars exhibits two main novel features compared to the fluvial case investigated by Colombini, Seminara & Tubino (1987): the basic flow is time periodic and the dominant form of sediment transport is typically transport in suspension rather than bedload transport. As in many other fields of hydrodynamic stability the time-periodic character of the basic flow will be seen to be readily accomodated in the theoretical approach and leads to a Floquet-type solution. Modelling transport in suspension will require the solution of a convection–diffusion equation coupled to the flow equations. As a result, unlike in the steady fluvial case (Colombini *et al.* 1987), a three-dimensional model will be employed.

The model will be formulated in the next section. In § 3 we summarize the basic solution for both the flow and concentration fields. In § 4 we formulate and solve the problem of linear stability of the basic tidal solution with respect to perturbations of the bar type. Results on the formative conditions of tidal bars are given in § 5 along with some discussion and concluding remarks.

2. Formulation of the problem

We consider a straight long channel connected at some initial cross-section with a tidal sea. The channel is assumed to have a rectangular cross-section, with constant width $2B$; hence, we neglect the slow spatial variation of channel width associated with channel convergence, its spatial scale being much larger than a typical bar wavelength. The banks of the channel are assumed to be non-erodible, while the bed is cohesionless, the sediment being uniform and the grain diameter d_s^* small enough for particles to be suspended by the turbulence generated by the propagation of the tidal wave throughout most of the tidal cycle. A star denotes a dimensional quantity subsequently made dimensionless.

Let us refer the flow field to a Cartesian coordinate system (x^*, y^*, z^*) with z^* vertical, x^* longitudinal and y^* transverse (see figure 3). Furthermore let a_0 be a scale for the amplitude of free-surface oscillations about the mean water level defined by the elevation H_0^* and denote by D_0^* a reference flow depth. We assume that, as it is

typical of many tidal environments, we can write

$$\epsilon = \frac{a_0}{D_0^*} \ll 1, \qquad \beta = \frac{B}{D_0^*} \gg 1. \tag{2.1a,b}$$

Typical values of ϵ in tidal channels of Venice Lagoon vary widely, ranging from values around 0.05 typical of the deeper channels up to values of order one characteristic of very shallow channels. Tidal channels are somewhat narrower than fluvial channels, exhibiting values of β which typically do not exceed 10 (see also figure 3 of Part 2).

We then make the relevant physical quantities dimensionless as follows:

$$(x^*, y^*) = B(x, y), \qquad (z^*, H^*, D^*) = D_0^*(z, H, D), \tag{2.2a,b}$$

$$(U^*, V^*, W^*) = V_0\left(U, V, \frac{W}{\beta}\right), \qquad P^* = \varrho V_0^2 P, \tag{2.2c,d}$$

$$t = \omega t^*, \qquad (\nu_T^*, \psi^*) = V_0 D_0^* \sqrt{C_{f0}}(\nu_T, \psi), \tag{2.2e,f}$$

having employed the following notation (see also figure 3): H^*, local free-surface elevation; D^*, local flow depth; (U^*, V^*, W^*), longitudinal, transverse and vertical components of the mean local velocity; P^*, mean pressure; t^*, time; ν_T^*, eddy viscosity; ψ^*, eddy diffusivity of suspended particles; ϱ, density of water; V_0, characteristic flow speed; ω, angular frequency of the tide; C_{f0}, reference friction coefficient. Typical values of the reference speed V_0^* range from about 0.5 to 1 $\mathrm{m\,s^{-1}}$. The reference friction coefficient C_{f0} attains typical values about $(2\text{–}5)\times 10^{-3}$.

Using the above dimensionless variables and a Boussinesq closure, the Reynolds equations are

$$\mathscr{L}U = -\frac{\partial P}{\partial x} + \beta\sqrt{C_{f0}}\frac{\partial}{\partial z}\left[\nu_T\frac{\partial U}{\partial z}\right], \tag{2.3}$$

$$\mathscr{L}V = -\frac{\partial P}{\partial y} + \beta\sqrt{C_{f0}}\frac{\partial}{\partial z}\left[\nu_T\frac{\partial V}{\partial z}\right], \tag{2.4}$$

$$0 = -\frac{\partial P}{\partial z} - \frac{1}{\mathscr{F}^2}, \tag{2.5}$$

$$\frac{\partial U}{\partial x} + \frac{\partial V}{\partial y} + \frac{\partial W}{\partial z} = 0, \tag{2.6}$$

with $\mathscr{L}$ the following differential operator:

$$\mathscr{L} \equiv \sigma_0\frac{\partial}{\partial t} + U\frac{\partial}{\partial x} + V\frac{\partial}{\partial y} + W\frac{\partial}{\partial z}. \tag{2.7}$$

The dimensionless parameters σ_0 and $\mathscr{F}^2$ are

$$\sigma_0 = \frac{\omega B}{V_0}, \qquad \mathscr{F}^2 = \frac{V_0^2}{gD_0^*}, \tag{2.8a,b}$$

where g is acceleration due to gravity.

Note that in (2.3)–(2.4) we have retained only the dominant components of the Reynolds stress tensor in the central region of the flow field (which excludes the side-wall boundary layers) where the appropriate lateral scale is channel width. Equation (2.5) simply states, in dimensionless form, that the mean pressure is hydrostatically distributed.

Furthermore, σ_0 represents the ratio between the time required for the flow to travel along a reach of length B and the tidal period. With typical values of B of the order of tens or hundreds of metres and V_0 about $1\,\mathrm{m\,s^{-1}}$, the value of σ_0 for a semidiurnal tide ($\omega = 1.4 \times 10^{-4}\,\mathrm{s^{-1}}$) falls roughly in the range 10^{-3}–10^{-2}. This suggests that inertial effects play a negligible role in flow processes occurring at the spatial scale of bars. Also note that in (2.3)–(2.6) we have neglected the effect of Coriolis forces, which turn out to scale with the inverse of the Rossby number $V_0/(\Omega B)$, where Ω is the angular frequency associated with Earth's rotation. Since Ω is comparable with ω, it turns out that the effect of Coriolis acceleration is as small as inertial effects in tidal channels.

The boundary conditions to be associated with equations (2.3)–(2.6) impose no slip at the bed, vanishing stresses at the free surface, and the requirement that the free surface must be a material surface:

$$U = V = W = 0 \qquad (z = H - D + z_o D), \tag{2.9a,b}$$

$$\left(\sigma_0 \frac{\partial}{\partial t} + U\frac{\partial}{\partial x} + V\frac{\partial}{\partial y}\right) H - W = 0 \qquad (z = H), \tag{2.10}$$

$$P = 0 \qquad (z = H), \tag{2.11}$$

$$\frac{\partial V}{\partial z} = 0 \qquad (z = H), \tag{2.12}$$

$$\frac{\partial U}{\partial z} = 0 \qquad (z = H), \tag{2.13}$$

with z_0 the dimensionless value of the conventional reference level for no slip under uniform flow conditions. Notice that, in writing (2.11)–(2.13), we have taken into account the nearly horizontal character of the free surface.

At the sidewalls we ignore the boundary layers and simply impose the flow to be tangential to the boundaries, hence

$$V = 0 \qquad (y = \pm 1). \tag{2.14}$$

A closure assumption for the eddy viscosity ν_T may be obtained assuming that the slow time variation of the flow field leads to a quasi-steady sequence of equilibrium states. Hence we write

$$\nu_T = \mathcal{N}(Z) u_* D, \tag{2.15}$$

where $\mathcal{N}(Z)$ is the distribution of eddy viscosity at equilibrium, with Z the normalized vertical coordinate:

$$Z = \frac{z - (H - D)}{D}. \tag{2.16}$$

Moreover u_* is a characteristic instantaneous value of a dimensionless friction velocity defined as $\sqrt{|\boldsymbol{\tau}^*|/(\varrho V_0^2 C_{f0})}$, with $\boldsymbol{\tau}^*$ the local and instantaneous component of the stress vector acting on the bottom in the tangential direction.

Mass balance of sediment transported as suspended load leads to a convection–diffusion equation for the volumetric sediment concentration $\mathscr{C}$:

$$\mathscr{L}\mathscr{C} - \beta W_s \frac{\partial \mathscr{C}}{\partial z} = \beta \sqrt{C_{f0}} \frac{\partial}{\partial z}\left[\psi \frac{\partial \mathscr{C}}{\partial z}\right], \tag{2.17}$$

with W_s the dimensionless value of the particle fall velocity defined in the form

$$W_s = \frac{W_s^*}{V_0}. \tag{2.18}$$

The typical size of sediments in tidal environments ranges about 0.1 mm, corresponding to a dimensional value of the settling speed of about $1\,\mathrm{cm\,s^{-1}}$. Hence its dimensionless value (2.18) is about 10^{-2}.

We point out that (2.17) is based on the assumption that the size and concentration of sediment particles are small enough for sediment to play an essentially passive role, being transported by the fluid except for the tendency of particles to settle (Lumley 1976).

The boundary conditions associated with (2.17) impose vanishing sediment flux at the sidewalls and at the free surface. Furthermore at the bed we impose the so-called 'gradient boundary condition' which essentially consists of an entrainment assumption whereby the net flux of sediment is assumed to be proportional to the difference between the actual local instantaneous concentration and the value that concentration would attain at equilibrium with the local and instantaneous flow conditions. The proportionality constant, i.e. the entrainment coefficient, is taken as usual to be equal to the particle velocity normal to the bed. The resulting form of the boundary conditions reads

$$\nabla\mathscr{C}\cdot\boldsymbol{n} = 0 \qquad (y = \pm 1), \tag{2.19}$$

$$[W_s\boldsymbol{k}\mathscr{C} + \sqrt{C_{fo}}\psi\nabla\mathscr{C}]\cdot\boldsymbol{n} = 0 \qquad (z = H), \tag{2.20}$$

$$[W_s\boldsymbol{k}\mathscr{C}_e + \sqrt{C_{fo}}\psi\nabla\mathscr{C}]\cdot\boldsymbol{n} = 0 \qquad (z = H - D + a_r D), \tag{2.21}$$

where ∇ is the dimensionless form of the gradient vector, $(1/\beta\partial/\partial x, 1/\beta\partial/\partial y, \partial/\partial z)$, $\boldsymbol{k}$ is the unit vector in the z-direction, $\boldsymbol{n}$ is the unit vector in the direction normal to the surface, $\mathscr{C}_e$ is the equilibrium value of bed concentration and $a_r = a_r^*/D_0^*$ is the conventional dimensionless value of the reference elevation where the boundary condition is imposed under uniform conditions. Several empirical expressions for $\mathscr{C}_e$ and a_r are available in the literature. They correlate $\mathscr{C}_e$ with a dimensionless measure of bottom stress, in the form of the so-called Shields parameter θ, and with particle Reynolds number R_p:

$$\theta = \frac{|\boldsymbol{\tau}^*|}{(\varrho_s - \varrho)g d_s^*}, \qquad R_p = \frac{\sqrt{(s-1)g d_s^{*3}}}{\nu}, \tag{2.22a,b}$$

where d_s^* and ϱ_s are diameter and density of sediment particles, $s = \varrho_s/\varrho$ and ν is kinematic viscosity. Typical values of θ in tidal environments may reach peaks up to 1–2.

A closure assumption for the eddy diffusivity ψ is also required. A line of reasoning similar to that which leads to (2.15) allows us to write

$$\psi = \Psi(Z)u_* D, \tag{2.23}$$

where $\Psi(Z)$ is the vertical distribution of eddy diffusivity at equilibrium.

The mathematical problem is finally closed by imposing the continuity equation for the sediment which governs the development of bottom perturbations. It may be written in the following form:

$$\frac{\sigma_0}{\beta}\mathscr{C}_M\frac{\partial(H-D)}{\partial t} + [W_s\boldsymbol{k}(\mathscr{C} - \mathscr{C}_e)\cdot\boldsymbol{n}]_{Z=a_r} + Q_0\left[\frac{\partial Q_{bx}}{\partial x} + \frac{\partial Q_{by}}{\partial y}\right] = 0, \tag{2.24}$$

where $\mathscr{C}_M$ is the packing concentration of the granular bed with value about 0.6, $\boldsymbol{Q}_b \equiv (Q_{bx}, Q_{by})$ is the bedload vector made dimensionless by means of the classical Einstein scale and Q_0 is the dimensionless parameter $[(\sqrt{(s-1)g d_s^{*3}})/V_0 B]$. Equation (2.24) requires a closure relationship for $\boldsymbol{Q}_b$ that can account for the influence of the sloping bed on particle trajectories. In fact, it is well known from the fluvial literature that on a sloping bottom the bedload deviates from the direction of bottom stress by an amount increasing with the local bed slope. In a linear context, like the one investigated in the next sections, it is fairly well established (see Kovacs & Parker 1994 and Talmon, Struiksma & van Mierlo 1995) that one may write

$$\boldsymbol{Q}_b = \phi_b \left\{ \frac{\boldsymbol{\tau}}{|\boldsymbol{\tau}|} - \frac{r}{\beta \theta^m} \frac{\partial (H-D)}{\partial y} \boldsymbol{j} \right\}, \tag{2.25}$$

where $\boldsymbol{j}$ is the unit vector in the y-direction, $\phi_b(\theta)$ is the intensity of bedload transport under equilibrium conditions while r and m are parameters for which various fairly equivalent values have been found on the basis of experimental observations. We follow Talmon *et al.* (1995) and take $r = 0.56$, $m = 1/2$.

The effect of longitudinal slope on bedload intensity is accounted for by introducing a corrected value $\hat{\theta}_c$ of the critical Shields stress in the form

$$\hat{\theta}_c = \theta_c - \frac{r_1}{\beta} \frac{\partial (H-D)}{\partial x}, \tag{2.26}$$

with r_1 empirical constant which is about 0.1.

The system (2.3)–(2.26) forms a closed set of equations which may be solved once expressions for $\mathscr{N}(Z)$, $\Psi(Z), C_{f0}$ and ϕ_b are known.

It will prove convenient in the following to employ the vertical coordinate Z scaled by the local flow depth, defined by (2.16). We then write:

$$\left(\frac{\partial}{\partial t}, \frac{\partial}{\partial x}, \frac{\partial}{\partial y}, \frac{\partial}{\partial z} \right) = \left(\mathrm{q}_t, \mathrm{q}_x, \mathrm{q}_y, \frac{1}{D} \frac{\partial}{\partial Z} \right), \tag{2.27}$$

having defined the operator $\mathrm{q}_j (j = t, x, y)$ in the form

$$\mathrm{q}_j = \frac{\partial}{\partial j} - \left[\frac{Z}{D} \frac{\partial D}{\partial j} + \frac{1}{D} \frac{\partial (H-D)}{\partial j} \right] \frac{\partial}{\partial Z}. \tag{2.28}$$

The momentum equation (2.5) with the boundary condition (2.11) is then readily solved to give the hydrostatic distribution for P:

$$P = \frac{D}{\mathscr{F}^2} (1 - Z). \tag{2.29}$$

Hence

$$\mathrm{q}_x P = \frac{\partial P}{\partial x} + \frac{1-Z}{D} \frac{\partial D}{\partial x} \frac{\partial P}{\partial Z} - \frac{1}{D} \frac{\partial H}{\partial x} \frac{\partial P}{\partial Z} = \frac{1}{\mathscr{F}^2} \frac{\partial H}{\partial x} \tag{2.30}$$

and

$$\mathrm{q}_y P = \frac{1}{\mathscr{F}^2} \frac{\partial H}{\partial y}. \tag{2.31}$$

The momentum and continuity equations (2.3)–(2.6) are then readily given the following form:

$$\mathrm{L}U = -\frac{1}{\mathscr{F}^2} \frac{\partial H}{\partial x} + \frac{\beta \sqrt{C_{f0}}}{D^2} \frac{\partial}{\partial Z} \left(\nu_T \frac{\partial U}{\partial Z} \right), \tag{2.32}$$

$$\mathrm{L}V = -\frac{1}{\mathscr{F}^2}\frac{\partial H}{\partial y} + \frac{\beta\sqrt{C_{f0}}}{D^2}\frac{\partial}{\partial Z}\left(\nu_T\frac{\partial V}{\partial Z}\right), \tag{2.33}$$

$$\mathrm{q}_x U + \mathrm{q}_y V + \frac{1}{D}\frac{\partial W}{\partial Z} = 0, \tag{2.34}$$

where

$$\mathrm{L} \equiv \sigma_0 \mathrm{q}_t + U\mathrm{q}_x + V\mathrm{q}_y + \frac{W}{D}\frac{\partial}{\partial Z}, \tag{2.35}$$

while the boundary conditions (2.9), (2.10), (2.12) and (2.13) become

$$U = V = W = 0 \qquad (Z = Z_0 = z_0), \tag{2.36a–c}$$

$$(\sigma_0 \mathrm{q}_t + U\mathrm{q}_x + V\mathrm{q}_y)H - W = 0 \qquad (Z = 1), \tag{2.37}$$

$$\frac{\partial U}{\partial Z} = \frac{\partial V}{\partial Z} = 0 \qquad (Z = 1). \tag{2.38a,b}$$

The convection–diffusion equation (2.17) takes the form

$$\mathrm{L}\mathscr{C} - \frac{W_s}{D}\frac{\partial \mathscr{C}}{\partial Z} = \frac{\beta\sqrt{C_{f0}}}{D^2}\frac{\partial}{\partial Z}\left[\psi\frac{\partial \mathscr{C}}{\partial Z}\right]. \tag{2.39}$$

This equation must be solved with the boundary conditions (2.19)–(2.21) where the gradient operator ∇ now reads

$$\nabla \equiv \left(\frac{\mathrm{q}_x}{\beta}, \frac{\mathrm{q}_y}{\beta}, \frac{1}{D}\frac{\partial}{\partial Z}\right). \tag{2.40}$$

Finally the bottom evolution equation keeps the form (2.24).

3. The local three-dimensional structure of the basic flow and concentration fields

The basic flow consists essentially of a tidal wave propagating in a long rectangular channel with slowly varying width. This is a subject which has recently received considerable attention (see in particular Friedrichs & Aubrey 1994; Lanzoni & Seminara 1998; and references therein).

However, for the scope of the present analysis, we do not need to know the solution for tide propagation in the whole channel, as the local flow structure at the spatial scale of bars is spatially uniform at the leading order of approximation. The interested reader is referred to the Appendix for a detailed derivation of the basic flow. Here it suffices to recall that for 'dissipative' tidal systems, that is when the dominant balance in the longitudinal momentum equation involves friction and gravity and local inertia is negligible, the basic flow (at the scale of bars) admits the simple lowest-order solution

$$U = U_0 = \bar{U}_0(t)F_0(Z), \tag{3.1}$$

$$H = 1, \tag{3.2}$$

$$D = 1, \tag{3.3}$$

$$\nu_T = \nu_{T0} = \mathscr{N}(Z)|\bar{U}_0(t)|, \tag{3.4}$$

where the function F_0 is the solution of the following differential problem:

$$\frac{\mathrm{d}}{\mathrm{d}Z}\left[\mathcal{N}(Z)\frac{\mathrm{d}F_0}{\mathrm{d}Z}\right] = -\sqrt{C_{f0}}, \tag{3.5}$$

$$F_0 = 0 \qquad (Z = Z_0), \tag{3.6}$$

$$\frac{\mathrm{d}F_0}{\mathrm{d}Z} = 0 \qquad (Z = 1). \tag{3.7}$$

Also note that the basic free-surface elevation and flow depth take the form (3.2) and (3.3) having taken the reference level at the average bottom and the reference flow depth as the average flow depth in the reach under consideration. Using Dean's (1974) structure for $\mathcal{N}(Z)$

$$\mathcal{N}(Z) = \frac{kZ(1-Z)}{1+2AZ^2+3BZ^3}, \qquad A = 1.84, \qquad B = -1.56, \tag{3.8a–c}$$

with k the von Kármán constant, we can integrate (3.5), with the boundary conditions (3.6)–(3.7), to obtain

$$F_0(Z) = \frac{\sqrt{C_{f0}}}{k}\left[\ln\frac{Z}{Z_0} + AZ^2 + BZ^3\right] \tag{3.9}$$

where

$$Z_0 = \exp\left(-\frac{k}{\sqrt{C_{f0}}} - 0.777\right). \tag{3.10}$$

Notice that the reference friction coefficient C_{f0} refers to the instant when $\bar{U}_0$ equals 1.

It is convenient to point out at this stage that the self-similar structure of the solution for U_0 is only valid provided local inertia in the momentum equation is negligible at the leading order of approximation. Otherwise the vertical distribution F_0 is itself time-dependent. Local inertia could be incorporated in the framework of the present analysis. However, as the non-self-similarity of the basic velocity distribution observed in real estuaries is a fairly weak effect, the essential features of bar formation in tidal channels are not likely to be significantly affected by such additional effect. However, a complete analysis will be required in order to conclusively substantiate that statement.

Also note that in principle any time dependence of the basic flow can be incorporated in the analysis through the function $\bar{U}_0(t)$. In particular one could readily account for the effect of overtides. For the sake of simplicity the stability analysis of the next section will be developed for the simple case

$$\bar{U}_0 = \cos t. \tag{3.11}$$

At the lowest order of approximation considered herein the structure of the basic concentration field $\mathscr{C}_0$ is readily obtained from (2.39) and (2.19)–(2.21). Recalling (2.23) we find

$$\psi = \psi_0 = \Psi(Z)|\bar{U}_0(t)|. \tag{3.12}$$

Hence, the following differential problem for $\mathscr{C}_0$ is obtained:

$$\left[\frac{\partial}{\partial Z}\left(\Psi(Z)\frac{\partial}{\partial Z}\right) + G(t)\frac{\partial}{\partial Z}\right]\mathscr{C}_0 = 0, \tag{3.13}$$

$$\Psi(Z)\frac{\partial \mathscr{C}_0}{\partial Z} + G(t)\mathscr{C}_{e0} = 0 \qquad (Z = a_r), \tag{3.14}$$

$$\Psi(Z)\frac{\partial \mathscr{C}_0}{\partial Z} + G(t)\mathscr{C}_0 = 0 \qquad (Z = 1), \tag{3.15}$$

where $C_{e0} = \mathscr{C}_e|_{\theta=\theta_0}$, with

$$\theta_0 = \bar{U}_0^2 \frac{C_{f0} V_0^2}{(s-1) g d_s^*} \tag{3.16}$$

and

$$G(t) = \frac{W_s}{|\bar{U}_0|\sqrt{C_{f0}}}. \tag{3.17}$$

The solution of this system is obtained in the form

$$\mathscr{C}_0 = \mathscr{C}_{e0} \exp\left[-\int_{a_r}^{Z} \frac{G(t)}{\Psi(Z)} \mathrm{d}Z\right] \tag{3.18}$$

and describes a Rouse-type distribution parametrically dependent on time.

4. Formation of bars: local theory

We now investigate the growth of perturbations of the flow and concentration fields associated with bottom perturbations of the bar type. As already pointed out in the previous section, the basic flow, the stability of which we wish to investigate, is slowly varying in the longitudinal direction due to the propagation of the tidal wave (and possibly to channel convergence). However, at the leading order examined in the present investigation we limit ourselves to a 'local' analysis, i.e. we neglect the effects of the 'slow' spatial variations of the basic flow on bar growth and we focus our attention on a reach of the estuary of length scaling on channel width.

Let us then consider a perturbed flow configuration of the form

$$(U, W, H, D, v_T) = (U_0, 0, 1, 1, v_{T0}) + \zeta(u_0, w_0, \mathscr{F}^2 h_0, d_0, v_{T0} n_0) E S_m + \text{c.c.} + O(\zeta^2), \tag{4.1}$$

$$V = \zeta[v_0 E C_m] + \text{c.c.} + O(\zeta^2), \tag{4.2}$$

where

$$\left.\begin{aligned} S_m &= \sin\left(m\tfrac{1}{2}\pi y\right), \quad C_m = \cos\left(m\tfrac{1}{2}\pi y\right), \quad (m \text{ odd}) \\ S_m &= \cos\left(m\tfrac{1}{2}\pi y\right), \quad C_m = \sin\left(m\tfrac{1}{2}\pi y\right), \quad (m \text{ even}) \end{aligned}\right\} (m = 1, 2, \ldots) \tag{4.3a–d}$$

$$E = \exp(\mathrm{i}\lambda x), \tag{4.3e}$$

where ζ is an infinitesimal parameter and c.c. denotes the complex conjugate of a complex number.

Furthermore from the dimensionless definition of v_T we readily find

$$n_0 = d_0 + \left(\frac{\partial u_0/\partial Z}{\partial U_0/\partial Z}\right)_{Z=Z_0}. \tag{4.4}$$

We then substitute from (4.1)–(4.4) into (2.32)–(2.38) and equate terms $O(\zeta)$ to derive a sequence of differential problems for v_0, w_0 and u_0.

The amplitude of the perturbation of the transverse component of velocity is the solution of the following problem:

$$\mathrm{L}_1 v_0 = \frac{\mu}{|\bar{U}_0|} h_0, \tag{4.5}$$

$$v_0 = 0 \quad (Z = Z_0), \tag{4.6}$$

$$\frac{\partial v_0}{\partial Z} = 0 \quad (Z = 1), \tag{4.7}$$

where L_1 is the differential operator

$$\mathrm{L}_1 \equiv \frac{\partial}{\partial Z}\left(\mathscr{N}\frac{\partial}{\partial Z}\right) - \Lambda I F_0 \tag{4.8}$$

and

$$\Lambda = \frac{\mathrm{i}\lambda}{\beta\sqrt{C_{f0}}}, \quad \mu = \frac{M}{\beta\sqrt{C_{f0}}}, \quad I = \frac{\bar{U}_0}{|\bar{U}_0|}, \quad M = (-1)^{m-1} m \tfrac{1}{2}\pi. \tag{4.9a–d}$$

The system (4.5)–(4.9) is readily solved in the form

$$v_0 = \frac{h_0}{|\bar{U}_0|}[v_2(Z) + c_V v_1(Z)], \qquad c_V = -\left(\frac{v_2'}{v_1'}\right)_{Z=1}, \tag{4.10a,b}$$

where a prime denotes the vertical derivative $\mathrm{d}/\mathrm{d}Z$, and the functions v_1 and v_2 are solutions of the initial value problems

$$\mathscr{L}_1 v_j = b_j \qquad (j = 1, 2), \tag{4.11}$$

$$v_j = 0 \quad (Z = Z_0) \qquad (j = 1, 2), \tag{4.12}$$

$$v_j' = 1 \quad (Z = Z_0) \qquad (j = 1, 2), \tag{4.13}$$

with

$$b_1 = 0, \qquad b_2 = \mu, \tag{4.14}$$

and $\mathscr{L}_1$ is the differential operator obtained from (4.8) on replacing $\partial/\partial Z$ by $\mathrm{d}/\mathrm{d}Z$. These problems are solved numerically.

Once v_0 is known, flow continuity (2.34) allows us to express w_0 in terms of u_0 as

$$w_0 = Mg - \mathrm{i}\lambda f + \mathrm{i}\lambda\bar{U}_0\left[F_0(Z-1)d_0 + \mathscr{F}^2 F_0 h_0 - d_0\int_{Z_0}^{Z} F_0(\tau)\mathrm{d}\tau\right], \tag{4.15}$$

where

$$g = \int_{Z_0}^{Z} v_0(\tau)\mathrm{d}\tau, \qquad f = \int_{Z_0}^{Z} u_0(\tau)\mathrm{d}\tau. \tag{4.16a,b}$$

Finally, employing all the above solutions, one derives the following differential problem for f:

$$\mathrm{L}_2 f = \frac{\Lambda}{|\bar{U}_0|} h_0 - \sqrt{C_{f0}}\bar{U}_0 d_0 - \Lambda|\bar{U}_0| d_0 F_0' \int_{Z_0}^{Z} F_0(\tau)\mathrm{d}\tau + I\mu F_0' g, \tag{4.17}$$

$$f = \frac{\partial f}{\partial Z} = 0 \qquad (Z = Z_0), \tag{4.18a,b}$$

$$\frac{\partial^2 f}{\partial Z^2} = 0 \qquad (Z = 1), \tag{4.19}$$

where L_2 is the following differential operator:

$$L_2 \equiv \frac{\partial}{\partial Z}\left(\mathcal{N}\frac{\partial^2}{\partial Z^2}\right) - \Lambda F_0 I\frac{\partial}{\partial Z} + \Lambda F_0' I - \left[\mathcal{N}\frac{\partial^2}{\partial Z^2}\right]_{Z_0}. \tag{4.20}$$

This problem is readily solved in the form

$$u_0 = \frac{h_0}{|\bar{U}_0|}[f_1' + c_{uh}f_0'] + |\bar{U}_0|d_0[f_2' + c_{ud}f_0'], \tag{4.21a}$$

$$c_{uh} = -\left(\frac{f_1''}{f_0''}\right)_{Z=1}, \qquad c_{ud} = -\left(\frac{f_2''}{f_0''}\right)_{Z=1}, \tag{4.21b,c}$$

where the functions $f_j (j = 0, 1, 2)$ are solutions of the following initial value problems:

$$\mathscr{L}_2 f_j = a_j \quad (j = 0, 1, 2), \tag{4.22}$$

$$f_j = f_j' = 0 \quad (Z = Z_0,\ j = 0, 1, 2), \tag{4.23}$$

$$f_j'' = 1 \quad (Z = Z_0,\ j = 0, 1, 2), \tag{4.24}$$

with

$$a_0 = 0, \quad a_1 = \Lambda + \mu F_0' I(g_2 + c_v g_1), \quad a_2 = -\left[\Lambda F_0' \int_{Z_0}^{Z} F_0(\tau)\mathrm{d}\tau + I\sqrt{C_{f0}}\right], \tag{4.25a–c}$$

and $\mathscr{L}_2$ is given by (4.20) with $\partial/\partial Z$ replaced by $\mathrm{d}/\mathrm{d}Z$. Finally at $O(\zeta)$ the kinematic boundary condition at the free surface (2.37) reads

$$w_0 = \mathrm{i}\lambda U_0 h_0 \mathscr{F}^2 \quad (Z = 1). \tag{4.26}$$

Using (4.10*a*), (4.15), (4.16) and (4.21*a*) expression (4.26) establishes the following relationship between h_0 and d_0:

$$h_0 = \bar{h}(t)\bar{U}_0|\bar{U}_0|d_0 \tag{4.27}$$

where

$$\bar{h}(t) = \frac{\mathrm{i}\lambda[1 + I(f_2 + c_{ud}f_0)]_{Z=1}}{[M(g_2 + c_v g_1) - i\lambda(f_1 + c_{uh}f_0)]_{Z=1}}. \tag{4.28}$$

Using (4.27)–(4.28) the whole solution for u_0, v_0, w_0 becomes simply proportional to the amplitude of the perturbation of flow depth d_0:

$$v_0 = \hat{v}(Z)\bar{U}_0(t)d_0, \qquad u_0 = \hat{u}(Z)\bar{U}_0(t)d_0, \qquad w_0 = \hat{w}(Z)\bar{U}_0(t)d_0, \tag{4.29a–c}$$

where $\hat{v}, \hat{u}$ and $\hat{w}$ are readily obtained from (4.10*a*), (4.15) and (4.21*a*). Note that the above solution, being proportional to $\bar{U}_0(t)$, varies smoothly in a neighbourhood of the instant of flow reversal.

Let us now proceed to evaluate the perturbation of the concentration field. Expand

$$(\mathscr{C}, \psi) = (\mathscr{C}_0, \psi_0) + \zeta\,[(\mathscr{C}_{10}, \psi_0 p_0)ES_m + \text{c.c.}] + O(\zeta^2), \tag{4.30}$$

with ζ infinitesimal. We note that the perturbation of eddy diffusivity leads to a relationship for p_0 identical with that obtained for n_0 (see (4.4)). Substituting from (4.30) into (2.39) and equating terms $O(\zeta)$, after some algebraic manipulations we eventually find

$$L_3\mathscr{C}_{10} = \Omega(Z, t)d_0, \tag{4.31}$$

where L_3 is the following differential operator:

$$L_3 \equiv \frac{\partial}{\partial Z}\left[\Psi \frac{\partial}{\partial Z}\right] - \Lambda I F_0 + G(t)\frac{\partial}{\partial Z}, \tag{4.32}$$

with G given by (3.17) and Ψ defined in (2.23).

Moreover, neglecting terms $O(\mathcal{F}^2)$, the function $\Omega(Z,t)$ reads

$$\Omega = \left\{ \frac{\hat{w} I}{\beta\sqrt{C_{f0}}} + \Lambda I F_0 (1 - Z) + G(t)\Gamma \right\} \frac{\partial \mathscr{C}_0}{\partial Z}, \tag{4.33}$$

where

$$\Gamma = \left(\frac{\hat{u}'}{F_0'}\right)_{Z=Z_0}. \tag{4.34}$$

The condition of vanishing flux at the free surface (2.20) at $O(\zeta)$ is found to be:

$$\left[\Psi \frac{\partial \mathscr{C}_{10}}{\partial Z} + G(t)\mathscr{C}_{10}\right]_{Z=1} = \Omega_1 d_0, \tag{4.35}$$

where

$$\Omega_1 = G\Gamma \mathscr{C}_0|_{Z=1}. \tag{4.36}$$

Similarly at the conventional reference level $Z = a_r$ the gradient boundary condition (2.21) at $O(\zeta)$ gives

$$\left[\Psi \frac{\partial \mathscr{C}_{10}}{\partial Z}\right]_{Z=a_r} = \Omega_0 d_0, \tag{4.37}$$

having expanded the Shields stress in the form

$$\theta = \theta_0 \left[1 + \zeta(2\Gamma d_0 E S_m + \text{c.c.}) + O(\zeta^2)\right] \tag{4.38}$$

and set

$$\Omega_0 = G\left[-2\theta_0 \left.\frac{\partial \mathscr{C}_e}{\partial \theta}\right|_{\theta_0,1} + \mathscr{C}_{e0}\right]\Gamma + I F_0|_{Z=a_r} \Lambda \mathscr{C}_{e0} + I \frac{\hat{w}|_{Z=a_r}}{\beta\sqrt{C_{f0}}}\mathscr{C}_{e0} - G \left.\frac{\partial \mathscr{C}_e}{\partial D}\right|_{\theta_0,1}. \tag{4.39}$$

The differential system (4.31)–(4.32), with the boundary conditions (4.35) and (4.37), is readily solved at each time in the form

$$\mathscr{C}_{10} = \hat{\mathscr{C}} d_0, \qquad \hat{\mathscr{C}} = c k_1 + k_2, \tag{4.40a,b}$$

where k_1, k_2 are solutions of the following initial value problems:

$$\mathscr{L}_3 k_j = r_j \qquad (j = 1,2), \tag{4.41a}$$

$$\Psi k_j' = e_j \qquad (Z = a_r) \quad (j = 1,2), \tag{4.41b}$$

$$k_j = \ell_j \qquad (Z = a_r) \quad (j = 1,2), \tag{4.41c}$$

with

$$r_1 = 0, \quad e_1 = 0, \quad \ell_1 = 1, \quad r_2 = \Omega, \quad e_2 = \Omega_0, \quad \ell_2 = 0. \tag{4.42a–f}$$

The constant c is

$$c = \frac{\Omega_1 - [\Psi k_2' + G k_2]_{Z=1}}{[\Psi k_1' + G k_1]_{Z=1}} \tag{4.43}$$

and $\mathscr{L}_3$ is given by (4.32) with $\partial/\partial Z$ replaced by $\mathrm{d}/\mathrm{d}Z$. The growth of perturbations

is eventually ascertained by solving the linearized form of the bottom evolution equation (2.24) which is found as

$$d_{0,t} = \mathscr{D}(t) d_0, \qquad \mathscr{D}(t) = \mathscr{D}_0(t) + \mathscr{D}_1(t), \tag{4.44a,b}$$

where

$$\mathscr{D}_1(t) = \frac{\beta W_s}{\sigma_0 \mathscr{C}_M} \left[-\bar{U}_0 \hat{\mathscr{C}}|_{Z=a_r} + 2\theta_0 \Gamma \left. \frac{\partial \mathscr{C}_e}{\partial \theta} \right|_{\theta_0,1} + \left. \frac{\partial \mathscr{C}_e}{\partial D} \right|_{\theta_0,1} \right], \tag{4.45}$$

$$\mathscr{D}_0(t) = \frac{\phi_{b0} Q_0}{\sigma_0 \mathscr{C}_M} \left\{ 2\mathrm{i}\lambda \Gamma I \phi_\theta - MI \left(\frac{\hat{v}'}{F_0'} \right)_{Z=Z_0} - \frac{rM^2}{\beta \sqrt{\theta_0}} - \frac{\lambda^2 r_1}{\beta \theta_0} \phi_\theta \right\}, \tag{4.46}$$

having set

$$\phi_{b0} = \phi_b(\theta_0), \tag{4.47}$$

$$\phi_\theta = \frac{\theta_0}{\phi_{b0}} \left. \frac{d\phi_b}{d\theta} \right|_{\theta_0}. \tag{4.48}$$

The marginal stability conditions are then obtained by setting

$$\int_t^{t+2\pi} \mathscr{D}(\tau) \mathrm{d}\tau = 0. \tag{4.49}$$

5. Results and discussion

In order to solve for the basic state and the perturbation fields we first need to provide convenient closure relationships for $\mathscr{C}_e, a_r, \Psi(Z), \phi_b$ and $\mathscr{C}_{f0}$.

Calculations were performed employing Van Rijn's (1984) closures for $\mathscr{C}_e$ and a_r:

$$\mathscr{C}_e = 0.015 \frac{d_s^*}{a_r^*} \left(\frac{\theta'}{\theta_c} - 1 \right)^{1.5} R_p^{-0.2}, \tag{5.1a}$$

$$a_r^* = \epsilon_e \qquad (\epsilon_e \geqslant 0.01 D^*), \tag{5.1b}$$

$$a_r^* = 0.01 D^* \qquad (\epsilon_e < 0.01 D^*), \tag{5.1c}$$

where θ' is the effective Shields stress acting on bedload particles, which is expressed in terms of the total Shields parameter θ using Engelund & Fredsøe's (1982) relationship:

$$\theta' = 0.06 + 0.3\theta^{3/2}. \tag{5.2}$$

Furthermore, ϵ_e is an effective roughness accounting for the effect of dunes, for which Van Rijn (1984) gives an expression which ultimately relates ϵ_e to bed shear stress, and θ_c is the critical Shields stress for sediment motion evaluated using Brownlie's (1981) relationship:

$$\theta_c = 0.22 R_p^{-0.6} + 0.06 \exp(-17.77 R_p^{-0.6}). \tag{5.3}$$

The eddy diffusivity is given McTigue's (1981) form

$$\left.\begin{aligned} \Psi &= 0.35Z \qquad (Z < 0.314), \\ \Psi &= 0.11 \qquad (0.314 \leqslant Z \leqslant 1). \end{aligned}\right\} \tag{5.4}$$

The intensity of bedload transport was evaluated using Meyer's-Peter & Muller's

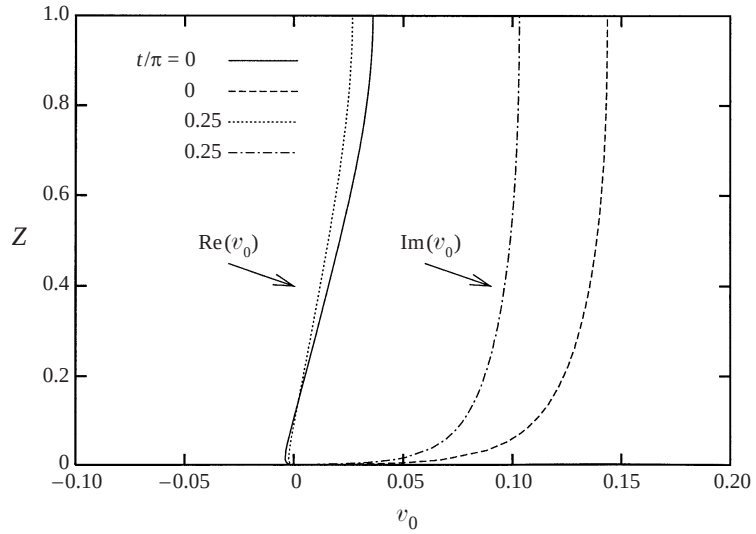

FIGURE 4. A typical vertical distribution of the real and imaginary parts of the lateral component of the perturbation velocity v_0 is plotted at two dimensionless times. Values of the relevant dimensionless parameters are: $\beta = 10$, $d_s = 2 \times 10^{-5}$, $R_p = 4$, $\lambda = 0.2$, $\bar{\theta}_0 = 1$, $d_0 = 1$.

classical relationship:

$$\phi_b = 8(\theta' - \hat{\theta}_c)^{3/2} \tag{5.5}$$

with $\hat{\theta}_c$ defined in (2.26).

Finally C_{f0} was calculated using Engelund & Hansen's (1967) formula, as modified by Engelund & Fredsøe (1982), which is able to account for the dissipative effect of dune-covered beds. Note that such an approach is based on the assumption that the dune pattern responds instantaneously to the forcing effect of the basic velocity field. This is only approximately true, as the actual response is qualitatively known to exhibit a small delay.

The simplest temporal distribution (3.11) of the cross-sectionally averaged velocity $\bar{U}_0(t)$, a harmonic tide, was assumed and the vertical distribution of the longitudinal component of the basic velocity field was then evaluated by means of (3.9).

We then proceeded to calculate the basic concentration field with the help of (3.16) and (3.17). The fall velocity W_s^* was evaluated using the following relationship which fits the experimental curve of Parker (1978):

$$\log_{10}\left(\frac{W_s^*}{\sqrt{(s-1)g d_s^*}}\right) = -1.181 + 0.966\pi_p - 0.1804\pi_p^2 + 0.003746\pi_p^3 + 0.0008782\pi_p^4, \tag{5.6}$$

with $\pi_p = \log_{10} R_p$.

The next step was to calculate the perturbation field. In particular we have solved for v_0 and u_0 using (4.11)–(4.14) and (4.22)–(4.25), respectively. The vertical component of the perturbation velocity w_0 was obtained by (4.15) and we finally calculated the quantity $\bar{h}$ as a function of time by means of (4.28). Figure 4 shows an example of the vertical distribution of the lateral component of the perturbation velocity v_0, for given values of the relevant dimensionless parameters and with $d_0 = 1$ (see (4.29*a*).

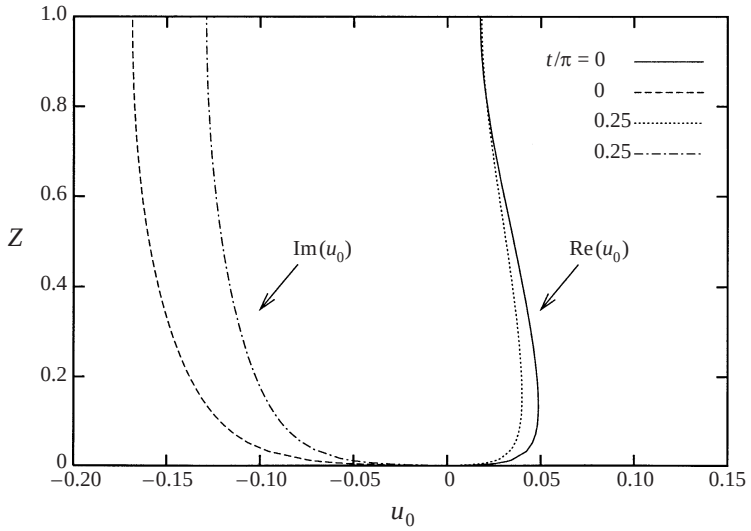

FIGURE 5. A typical vertical distribution of the real and imaginary parts of the longitudinal component of the perturbation velocity u_0 is plotted at two dimensionless times. Values of the relevant dimensionless parameters are: $\beta = 10$, $d_s = 2 \times 10^{-5}$, $R_p = 4$, $\lambda = 0.2$, $\bar{\theta}_0 = 1$, $d_0 = 1$.

Note that the solution for v_0 satisfies the condition

$$v_0(Z\,;t) = \tilde{v}_0(Z\,;t + \pi), \tag{5.7}$$

where a tilde denotes the complex conjugate. Hence the vertical distribution of the lateral component of the perturbation velocity is insensitive to the sign of the basic velocity, as one expects on physical grounds given the symmetry of the problem within the present scheme. Figure 5 shows an example of the vertical distribution of the longitudinal component of the perturbation velocity $u_0(Z\,;t)$ at different times.

The next step was to obtain the perturbation of the concentration distribution $\mathscr{C}_{10}$ by means of (4.40)–(4.43): an example of the vertical distribution of $\mathscr{C}_{10}$ at different times is reported in figure 6. Note that all the above initial value problems were solved numerically using a Runge–Kutta scheme of fourth order.

Once the perturbation field was known, we evaluated the function $\mathscr{D}(t)$ and its integral over a cycle, i.e. the complex bar growth rate. For given values of the peak basic Shields stress $\bar{\theta}_0$, particle Reynolds number R_p and relative roughness $d_s = d_s^*/D_0^*$, searching for the marginal stability conditions, characterized by vanishing value of the real part of the complex growth rate, allowed us to construct neutral stability curves in the plane (λ, β) for each transverse mode m.

The major distinct effect of the uniform geometry of the channel and of the periodicity of the basic flow with vanishing mean is to let the imaginary part of $\mathscr{D}(t)$ be such that its integral over a tidal cycle is invariably found to vanish. This is not surprising. In fact the physical implication of this result is that, unlike river bars, tidal bars do not exhibit a net migration over a tidal cycle. Note that this does not imply that bars do not migrate but, rather, that they migrate alternately forward and backward in a symmetric fashion. In other words tidal bars are not instantaneously steady features but they are steady features in the mean.

In figure 7 we have plotted the instantaneous value of the growth rate through a quarter of a tidal cycle for four different values of the bar wavenumber. This

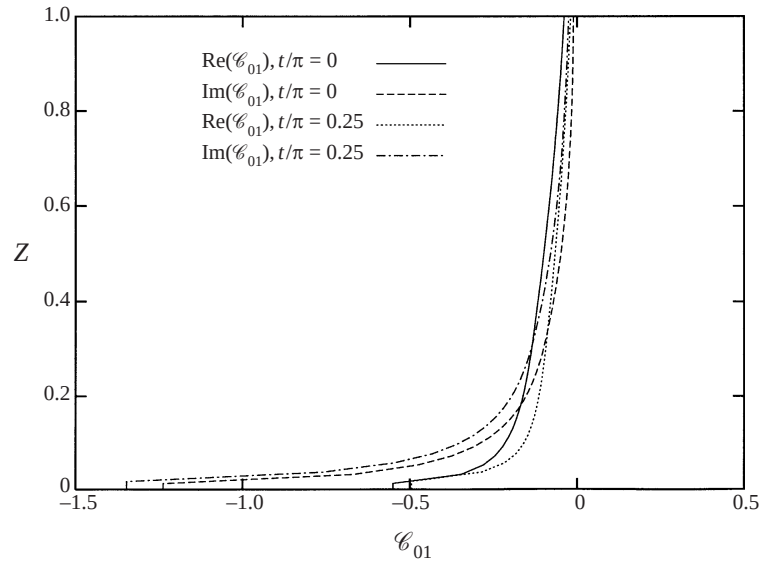

FIGURE 6. A typical vertical distribution of the real and imaginary parts of the perturbation of sediment concentration is plotted at two different times. Values of the relevant dimensionless parameters are: $\beta = 10$, $\lambda = 0.5$, $d_s = 2 \times 10^{-5}$, $R_p = 4$, $\lambda = 0.2$, $\bar{\theta}_0 = 1$, $d_0 = 1$.

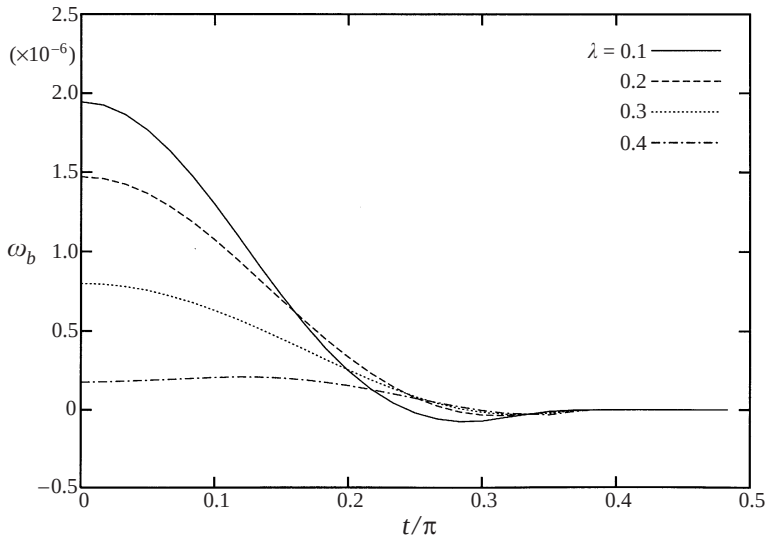

FIGURE 7. The temporal distribution of the instantaneous value of the bar growth rate ω_b is plotted for different values of the bar wavenumber λ. Values of the relevant parameters are: $\beta = 10$, $R_p = 4$, $d_s = 2 \times 10^{-5}$, $\bar{\theta}_0 = 1$.

figure clarifies how bar growth arises from an integrated effect of the bar growth rate throughout the tidal cycle.

The marginal stability curve of the first mode (alternate bar mode) is given in figure 8. Note its close similarity with the corresponding curve obtained by Colombini *et al.* (1987) in the steady (river) case. Figure 8 shows that increasing the Shields stress gives rise to interesting additional features of the problem. A major effect displayed

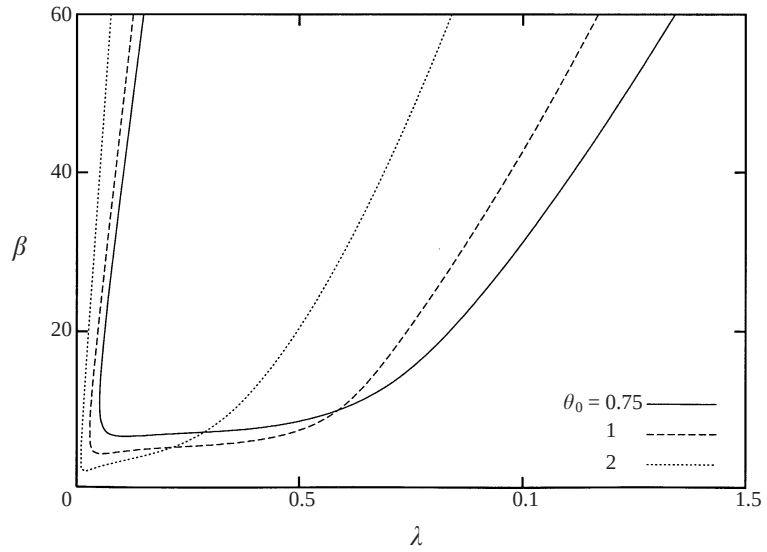

FIGURE 8. Marginal stability curves for different values of peak Shields stress ($R_p = 4$, $d_s = 0.00002$).

by the present results is the destabilization associated with large values of the Shields stress, displayed by the decrease of the critical value of the width to depth ratio. Note that this effect is mainly due to the decreasing stabilizing role played by gravity, but its effect is somewhat counteracted by suspended load, which plays a stabilizing role at sufficiently large wavenumbers. This finding agrees with results obtained in the steady fluvial case (Tubino, Repetto & Zolezzi 1999). Let us analyse this effect in physical terms.

Consider first the case of negligible suspended load. The picture, here, is quite similar to the steady case discussed in detail by Colombini *et al.* (1987). The growth rate has two contributions. One is proportional to $-\sin\delta_1$, with δ_1 the phase lag between the perturbation of the longitudinal component of bedload flux and the perturbation of bottom elevation, and is linearly proportional to the amplitude of the longitudinal component of the perturbation of the bedload flux vector, which is an increasing function of Shields stress. This contribution is quite similar to the corresponding contribution found in the analysis of dune formation (Engelund & Fredsoe 1982) and is invariably destabilizing, though with decreasing rate as bar wavenumber λ tends either to zero or to infinity, since δ_1 is found to vary from π to 2π as λ varies in the range $(0, \infty)$. Hence, this contribution to the growth rate increases, for given λ, as Shields stress increases and exhibits a peak for some finite value of λ for given Shields stress. Moreover it is found to be only weakly dependent on the aspect ratio of the channel.

The second contribution to the growth rate is proportional to $\cos\delta_2$, with δ_2 the phase lag between the perturbation of the transverse component of bedload flux and the perturbation of bottom elevation. The proportionality constant is linearly proportional to the parameter m describing the order of the transverse mode (see (4.3*a–d*)) and to the amplitude of the transverse component of the perturbation of the bedload flux vector. Due to the effect of gravity this contribution is invariably stabilizing. In fact δ_2 is found to vary from π to $\pi/2$ as λ varies in the range $(0, \infty)$; however, the intensity of this stabilizing effect is a decreasing function of Shields

stress and has a dominant contribution which is inversely proportional to the width ratio β, as suggested by (2.25).

As a result of the above behaviour, in the absence of suspended load, the growth rate tends to vanish as λ tends either to zero or to infinity for any value of the Shields stress and of the width ratio. For low enough values of β the first contribution never exceeds the second and the basic flat bed keeps stable. If a threshold value of β is exceeded, an unstable range is detected and a most unstable wavenumber is selected. On the other hand, as the Shields stress increases, the stabilizing contribution decreases monotonically: hence, in the mathematical limit for the Shields parameter tending to infinity, the basic state is unstable for any λ.

The inclusion of suspended load changes the picture in a way similar to that discussed by Tubino *et al.* (1999) for the fluvial case. Suspended load essentially adds a third contribution to the growth rate, which may be written in a form quite similar to that of the first (destabilizing) contribution, hence proportional to $-\sin\delta_3$, with δ_3 the phase lag between the perturbation of the longitudinal component of suspended load flux and the perturbation of bottom elevation. Again, the coefficient of proportionality is linearly proportional to the amplitude of the longitudinal component of the perturbation of the suspended load flux vector, which is also an increasing function of Shields stress. The phase lag δ_3 mainly arises from the effect of longitudinal convection of suspended sediments, hence it depends on the bar wavenumber λ. It turns out that the contribution of suspended load to the bar growth rate (which includes a further, minor, effect associated with the transverse component of suspended load), shifts from positive (destabilizing) to negative (stabilizing) as λ increases. This finding corresponds to the physical fact that the peak of the longitudinal component of suspended load shifts from the fourth to the first quadrant as λ increases. It is then not surprising that, as Shields stress increases and suspended load becomes dominant relative to bedload, the marginal stability curves shift towards the vertical axis, while the critical values of both the width ratio and bar wavenumber decrease.

It is worth noticing that alternative forms of the relationship for the reference concentration $\mathscr{C}_e$, though affecting quantitatively the bar growth rate, do not seem to alter qualitatively the picture outlined above: this is shown in figure 9 where a comparison is reported between marginal stability curves obtained through different closures for $\mathscr{C}_e$.

In figure 10 we have plotted the bar wavenumber characterized by the maximum growth rate $\lambda_{\max}$ for different values of the peak Shields stress and given values of the particle Reynolds number R_p and relative roughness.

It is a tedious exercise left to reader to show that the condition (4.49) is invariant with respect to the order m of the transverse mode once we set the following transformation:

$$\beta_{cm} = m\beta_{c1}, \qquad \lambda_{cm} = m\lambda_{c1}, \tag{5.8a,b}$$

where $\beta_{cm}(m = 1, 2, \ldots)$ is the critical value of the width to depth ratio characteristic of mode m and λ_{cm} is the corresponding critical wavenumber. Note that (5.8) imply that at large values of the Shields stress, when β_{c1} tends to vanish, all the modes tend to be simultaneously excited, though with unequal growth rate. This suggests that the bar pattern actually observed under these conditions may arise from some non-obvious nonlinear competition among different modes, which may only be described by means of a fully nonlinear analysis.

Various effects ignored in the present investigation will deserve attention in the

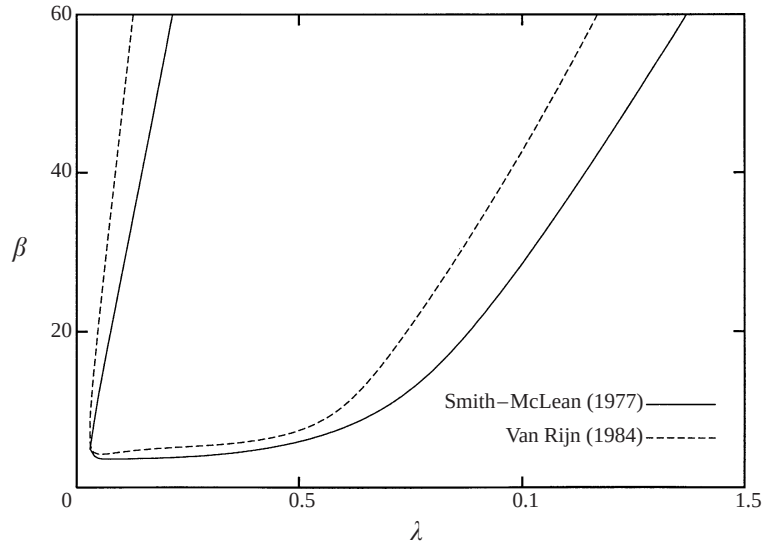

FIGURE 9. Marginal stability curves obtained through different closure relationships for the reference concentration $\mathscr{C}_e$. Values of the relevant parameters are: $R_p = 4, d_s = 2 \times 10^{-5}, \bar{\theta}_0 = 1$. The reference level a_r^* is set according to $(5.1b, c)$ and $\gamma_0 = 0.0024$ in Smith and McLean (1977) formula.

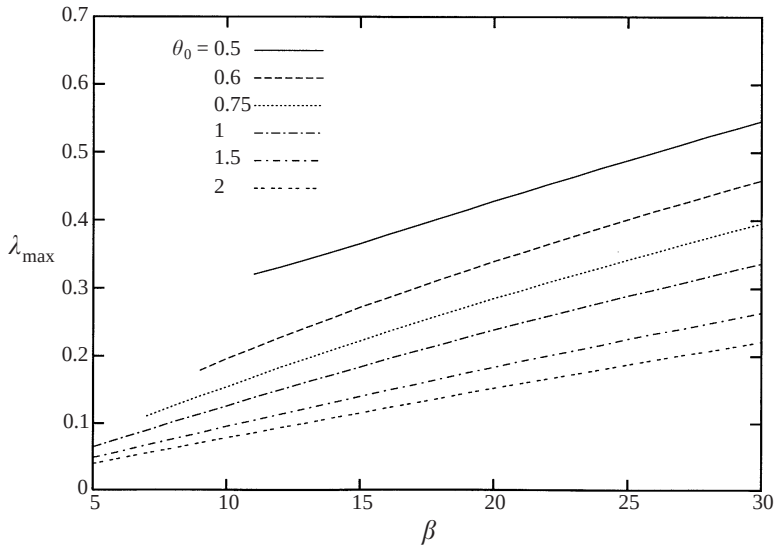

FIGURE 10. The wavenumber $\lambda_{\max}$ characterized by maximum growth is plotted versus the width ratio for different values of the peak Shields stress ($R_p = 4$, $d_s = 0.00002$).

future. We have ignored the slow spatial variation of the basic flow, arising from the propagation of the tidal wave in the slowly converging channel. This additional feature may be accounted for by employing a WKBJ type of asymptotic analysis.

Furthermore in the present analysis we have assumed the local inertia to be negligible at leading order: as a result the basic flow had a self-similar structure. Removing this hypothesis implies that the vertical distributions of basic flow and

concentration fields vary in time throughout the tidal cycle. This in turn affects the perturbation field and may alter the bar instability process.

Finally, let us clarify the relationship between our work and the work of Schuttelaars & de Swart (1999) (hereinafter referred to as SdS); they differ in many respects. First, SdS investigate the formation of bars in tidal channels of length assumed to be small with respect to the tidal wavelength and consider bed perturbations scaling on the finite channel length. They find that the bottom elevation of the basic state increases linearly landward, unlike the present case where, at the scale of bars, bottom elevation is constant at leading order in the basic state. As a result, whereas in the present solution the longitudinal wavenumber may take any real positive value, in SdS a discrete number of longitudinal modes is associated with the finite length of the channel. Furthermore, the spatial uniformity of our basic state (at the scale of bars) leads to a Fourier structure of perturbations, which is not the case in SdS. Moreover, we do not need to fit end conditions in the present work as the bar wavelength scales with channel width and the bar structure is slowly varying in the longitudinal direction, the channel length being much larger than the bar wavelength.

We feel that, in principle, by letting the channel length tend to infinity in SdS's analysis, the most unstable mode should tend to that predicted in the present work, just like the structure of Taylor vortices between cylinders of finite length tends to the classical uniform distribution as the length becomes large enough. On the other hand, in practice, the above comparison cannot be pursued as the model employed by SdS is significantly different from ours in several aspects.

We have employed a three-dimensional model of both the flow and concentration fields which has allowed us to predict the phase lag of suspended load relative to the bottom perturbation, leading to bar stabilization in the high-wavenumber range. On the other hand SdS employ a two-dimensional model unable to describe that effect.

In SdS advective terms are neglected in the momentum equations, an approximation which is said to be ".... the consequence of the assumption of a short embayment ....". Owing to such approximation the validity of SdS's model cannot be extended to cover modes of wavelength of the order of a few channel widths. Note that the most unstable longitudinal mode in figure 13 of SdS is characterized by a value of ℓn of about 70. In our notation ℓn is $n\pi L/B$, hence modes higher than the second would correspond to a ratio of channel length L to channel width B smaller than 10.

Various other approximations, like the linearization of the frictional term extended to the range where the flow depth tends to vanish and the adoption of the boundary condition of inerodible bed at the bay entrance, make any attempt to compare results of SdS with the present results not feasible.

This work has been developed in the framework of the National Project cofunded by MURST and Universities of Genova and Trento 'Morfodinamica fluviale e costiera'. A preliminary version of the present work was presented at PECS '96 (Seminara & Tubino 1998).

Appendix. The basic flow

In order to derive the local structure of the basic flow we define a suitable dimensionless longitudinal coordinate ξ

$$\xi = \gamma x, \tag{A 1}$$

where

$$\gamma \equiv \frac{B}{L} \ll 1, \tag{A 2}$$

and L is the spatial scale of the tidal wave. Note that we ignore any further slow spatial dependence associated with channel convergence and restrict ourselves to the leading-order representation of basic flow; hence we ignore the lateral component of the basic velocity field. Since

$$\frac{\partial}{\partial x} = \gamma \frac{\partial}{\partial \xi}, \tag{A 3}$$

the balance (2.34) implies that

$$W \sim O(\gamma). \tag{A 4}$$

The appropriate choice for the velocity scale V_0 then arises from the dominant balance in (2.37). Since

$$\frac{\sigma_0}{U} \frac{\partial H/\partial t}{\partial H/\partial x} \sim O\left(\frac{\sigma_0}{\gamma}\right) = \frac{\omega L}{V_0} \tag{A 5}$$

and the flow speed V_0 is typically much smaller than the wave speed (ωL), it follows that the terms balancing in (2.37) are W and $\sigma_0 \partial H/\partial t$. Hence we require that

$$\sigma_0 \frac{a_0}{D_0^*} = \gamma. \tag{A 6}$$

Recalling (2.8*a*), the condition (A 6) leads to the following expression for V_0:

$$V_0 = \omega L. \tag{A 7}$$

Based on (A 4) we then rescale U and W in the form

$$U = U_0, \qquad W = \gamma W_0, \tag{A 8a, b}$$

where U_0 and W_0 are functions of ξ, t and Z, and we rewrite the governing equations (2.32)–(2.34) in a form appropriate for the analysis of the basic flow:

$$\frac{1}{D} \frac{\partial W_0}{\partial Z} = -q_\xi U_0, \tag{A 9}$$

$$\mathrm{L}_0 U_0 = -\frac{\gamma}{\mathscr{F}^2} \frac{\partial H}{\partial \xi} + \frac{\beta \sqrt{C_{f0}}}{D^2} \frac{\partial}{\partial Z}\left(\nu_T \frac{\partial U_0}{\partial Z}\right), \tag{A 10}$$

where D is an $O(1)$ quantity and L_0 is the following linear partial differential operator:

$$\mathrm{L}_0 \equiv \frac{\gamma}{\epsilon} q_t + \gamma U_0 q_\xi + \gamma \frac{W_0}{D} \frac{\partial}{\partial Z}. \tag{A 11}$$

Similarly the boundary conditions (2.36)–(2.38) take the following form:

$$U_0 = W_0 = 0 \qquad (Z = Z_0), \tag{A 12a, b}$$

$$\frac{\partial U_0}{\partial Z} = 0 \qquad (Z = 1), \tag{A 13}$$

$$\frac{1}{\epsilon} \frac{\partial H}{\partial t} + U_0 \frac{\partial H}{\partial \xi} - W_0 = 0 \qquad (Z = 1). \tag{A 14}$$

We now assume that the dominant balance in the longitudinal momentum equation (A 10) involves friction and gravity. Since perturbations of free-surface elevation

relative to the still water level are $O(\epsilon)$, we set

$$\frac{\gamma\epsilon}{\mathscr{F}^2} = \beta C_{f0}. \tag{A 15}$$

The conditions (A 6), (A 15) determine the velocity scale V_0 in the form

$$V_0 = \left(\frac{g a_0^2 \omega}{C_{f0}}\right)^{1/3}. \tag{A 16}$$

The length scale L is then readily obtained from (A 7). We also assume that local inertia is negligible at leading order. Comparison between the orders of magnitude of gravity and local inertia in (A 10) shows that this assumption is valid provided the following condition is satisfied:

$$\mathscr{F}^2 \ll \epsilon^2. \tag{A 17}$$

As discussed by Lanzoni & Seminara (1998) (A 17) is approximately satisfied by some estuaries. Under the above hypotheses the system (A 9–A 10) admits the simplest lowest-order solution:

$$U_0 = \bar{U}_0(t,\xi)F_0(Z), \tag{A 18}$$

$$W_0 = \bar{U}_0(t,\xi)G_0(Z), \tag{A 19}$$

$$(H, D) = [H_0, D_0(\xi)] + \epsilon\,[H_1(\xi,t), D_1(\xi,t)]\,, \tag{A 20}$$

$$\nu_T = \mathscr{N}(Z)|\bar{U}_0(\xi,t)|D_0. \tag{A 21}$$

Substituting from (A 18)–(A 21) into (A 10), where inertial terms are neglected, we obtain

$$\bar{U}_0|\bar{U}_0|\frac{\mathrm{d}}{\mathrm{d}Z}\left[\mathscr{N}(Z)\frac{\mathrm{d}F_0}{\mathrm{d}Z}\right] = \left(\frac{\gamma\epsilon}{\mathscr{F}^2\beta\sqrt{C_{f0}}}\right)D_0\frac{\partial H_1}{\partial\xi} = \sqrt{C_{f0}}D_0\frac{\partial H_1}{\partial\xi}. \tag{A 22}$$

Recalling the boundary condition (A 13), equation (A 22) can be integrated once to give

$$-\bar{U}_0|\bar{U}_0|\left(\mathscr{N}(Z)\,\frac{\mathrm{d}F_0}{\mathrm{d}Z}\right)\Bigg|_{Z_0} = D_0\frac{\partial H_1}{\partial\xi}\sqrt{C_{f0}}. \tag{A 23}$$

Recalling that, by definition, $(\mathscr{N}(Z)\mathrm{d}F_0/\mathrm{d}Z)|_{Z_0}$ is equal to $\sqrt{C_{f0}}$, from (A 23) we find:

$$D_0\frac{\partial H_1}{\partial\xi} + \bar{U}_0|\bar{U}_0| = 0. \tag{A 24}$$

This equation is the lowest-order approximation of the one-dimensional formulation of the momentum equation arising in the present framework.

The continuity equation (2.34) at lowest order reads

$$\frac{\partial U_0}{\partial\xi} + \frac{(1-Z)}{D_0}\frac{\partial D_0}{\partial\xi}\frac{\partial U_0}{\partial Z} + \frac{1}{D_0}\frac{\partial W_0}{\partial Z} = 0, \tag{A 25}$$

which may be integrated at once, with the boundary condition (A12*b*), to give

$$W_0|_{Z=1} + \frac{\partial}{\partial\xi}(\bar{U}_0 D_0) = 0. \tag{A 26}$$

The quantity $W_0|_{Z=1}$ is obtained from the lowest-order approximation of the boundary

condition (A 14) and is equal to $\partial H_1/\partial t$; hence (A 26) reduces to the classical one-dimensional form of the continuity equation

$$\frac{\partial H_1}{\partial t} + \frac{\partial}{\partial \xi}(\bar{\mathrm{U}}_0 D_0) = 0. \tag{A 27}$$

The vertical structure of W_0, i.e. the function $G_0(Z)$, is then obtained by integrating (A 25).

The system of equations (A 24), (A 27) can be readily solved (Lanzoni & Seminara 1998) in the fully nonlinear case. Note however that at the lowest order of approximation the basic flow 'felt' by bars is spatially uniform, i.e. purely time dependent. More precisely the quantity H_1 does not enter the analysis, and we may choose the local average flow depth as reference depth to set $D_0 = 1$ and expand:

$$\bar{U}_0 = \bar{U}_0(t)[1 + O(\gamma)]. \tag{A 28}$$

Finally, using (2.24), one can show that, at leading order, bottom elevation undergoes periodic oscillations around a flat equilibrium state with dimensionless amplitudes of order $(W_s^* \mathscr{C}/\omega D_0^*)$ which may attain values of about 10^{-4}, small enough to be safely ignored.

REFERENCES

Barwis, J. 1978 Sedimentology of some South Carolina tidal-creek point bars, and a comparison with their fluvial counterparts. In *Fluvial Sedimentology* (ed. A. D. Miall), pp. 128–160 Geological Survey of Canada.

Brownlie, W. R. 1981 Prediction of flow depth and sediment discharge in open channels. *Rep.* KH-R-43A. W.M. Keck Laboratory, Cal. Inst. Techn., Pasadena.

Colombini, M., Seminara, G. & Tubino, M. 1987 Finite-amplitude alternate bars. *J. Fluid Mech.* **181**, 213–232.

Dalrymple, R. W. & Rhodes, R. M. 1995 Estuarine dunes and bars. In *Geomorphology and Sedimentology of Estuaries* (ed. G. M. E. Percillo). Developments in Sedimentology, vol. **53**, pp. 359–422. Elsevier.

Dean, R. B. 1974 *Aero Rep.* 74-11. Imperial College, London.

Engelund, F. & Fredsøe, J. 1982 Sediment ripples and dunes. *Ann. Rev. Fluid Mech.* **14**, 13–37.

Engelund, F. & Hansen, E. 1967 *A Monograph on Sediment Transport in Alluvial Streams.* Copenhagen: Danish Technical Press.

Friedrichs, C. T. & Aubrey, D. G. 1994 Tidal propagation in strongly convergent channels. *J. Geophys. Res.* **99**, 3321–3336.

Kovacs, A. & Parker, G. 1994 A new vectorial bedload formulation and its application to the time evolution of straight river channels. *J. Fluid Mech.* **267**, 153–183.

Lanzoni, S. & Seminara, G. 1998 On tide propagation in convergent estuaries. *J. Geophys. Res.* **103**, C13, 793–812.

Lumley, J. L. 1976 Two-phase and non-Newtonian flows. In *Turbulence* (ed. P. Bradshaw). Springer.

McTigue, D. F. 1981 Mixture theory for suspended sediment transport. *J. Hydr. Div. ASCE* **107**, HY6, 659–673.

Parker, G. 1978 Self formed rivers with stable banks and mobile bed. Part l. The sand-silt river. *J. Fluid Mech.* **89**, 109–125.

Schuttelaars, H. M. & Swart, H de. 1999 Initial formation of channels and shoals in a short tidal embayment. *J. Fluid Mech.* **386**, 15–42 (referred to herein as SdS).

Seminara, G. 1995 Invitation to river morphodynamics. In *Nonlinear Dynamics and Pattern Formation in Natural Environment* (ed. A. Doelman & A. van Harten), pp. 269–294. Pitman Research Notes in Mathematics, ser. 335, Longman.

Seminara, G. & Tubino, M. 1998 On the formation of estuarine free bars. In *Physics of Estuaries and Coastal Seas* (ed. J. Dronkers & M. Scheffers), pp. 345–353, A. A. Balkema.

Smith, J. D. & McLean, S. R. 1977 Spatially averaged flow over a wavy surface. *J. Geophys. Res.* **82**, 1735–1746.

Solari, L., Seminara, G., Lanzoni, S., Marani, M. & Rinaldo, A. 2001 Sand bars in tidal channels. Part 2. Tidal meanders. Submitted for publication to *J. Fluid Mech.*

Talmon, A. M., Struiksma, N. & Mierlo C. L. M. van 1995 Laboratory measurements of the direction of sediment transport on transverse alluvial-bed slopes. *J. Hydraul. Res.* **33**, 519–534.

Tubino, M., Repetto, R. & Zolezzi, G. 1999 Free bars in rivers, *J. Hydraul. Res.* **37**, 759–775.

Van Rijn, L. C. 1984 Sediment transport. Part Il. Suspended load transport. *J. Hydraul. Engng. ASCE* **110**, 1613–1641.